Available online at www.sciencedirect.com
ScienceDirect
Metamaterials 4 (2010) 112–118
Metamaterials
www.elsevier.com/locate/metmat

Focusing of electromagnetic radiation by a flat slab of a crossed wire mesh metamaterial

Tiago A. Morgado, Mário G. Silveirinha *

Universidade de Coimbra, Instituto de Telecomunicações, Departamento de Engenharia Electrotécnica, Pólo II, 3030 Coimbra, Portugal

Received 21 November 2009; received in revised form 4 February 2010; accepted 15 February 2010
Available online 21 February 2010

Abstract

In this work, we numerically demonstrate electromagnetic focusing using a spatially dispersive metamaterial. Based on the phenomenon of broadband all-angle negative refraction by a crossed wire mesh, it is demonstrated that a flat slab of the metamaterial enables partial focusing of *p*-polarized electromagnetic radiation. The reported results are supported by full wave simulations and by analytical calculations based on homogenization theory.

PACS: 42.70.Qs; 78.20.Ci; 41.20.Jb; 78.66.Sq

Keywords: Negative refraction; Focusing; Spatial dispersion; Wire media

1. Introduction

The phenomenon of negative refraction has received a great attention in recent years due to its unique implications in the image formation and in the manner how it is perceived by the human brain, and also because its theoretical description required the revision of classical geometrical optics. The light refracted in materials exhibiting negative refraction obeys a reversed Snell's law, so that the refracted wave emerges on the same side of the surface normal as the incident wave, in contrast to what happens in usual materials (e.g., glass). This remarkable effect has interesting implications in a broad range of optical devices, being perhaps the possibility of focusing a divergent beam of rays with a flat lens one of the most attractive applications.

Negative refraction using double negative materials was first predicted by Veselago [1] in 1968. In his early paper, it was theoretically demonstrated that materials with simultaneously negative permittivity and permeability (negative index of refraction) may enable negative refraction and consequently the focusing of electromagnetic radiation by a flat lens. Many years later, Pendry has further investigated this concept [2], predicting that besides focusing "light rays" such double negative medium also produces flawless images with super-resolution: a perfect lens. Such ideas stimulated the realization of artificially structured materials (metamaterials) with unusual electromagnetic properties, and in 2001 the negative refraction property was experimentally verified at microwaves [3]. The concept of negative refraction based on double negative metamaterials was recently demonstrated in the optical domain [4].

Despite all the remarkable potentials of low-loss media with a negative isotropic index of refraction, the realization of this kind of materials is technologically challenging, and it remains today a promise for the future. Hence, researchers have explored alterna-

* Corresponding author. Tel.: +351 239 796268; fax: +351 239 796293.
E-mail addresses: tiago.morgado@co.it.pt (T.A. Morgado), mario.silveirinha@co.it.pt (M.G. Silveirinha).

1873-1988/$ – see front matter © 2010 Elsevier B.V. All rights reserved.
doi:10.1016/j.metmat.2010.02.002

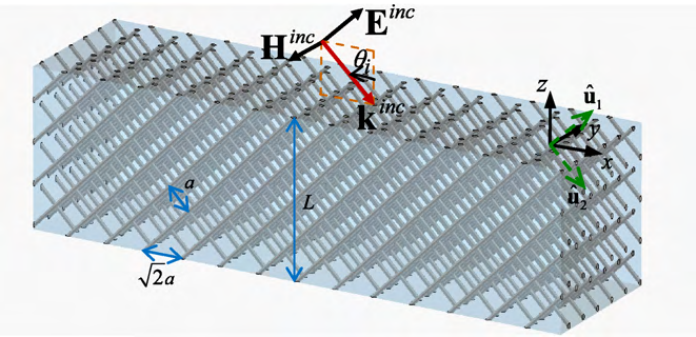

Fig. 1. Geometry of the crossed wires metamaterial, formed by two orthogonal arrays of nonconnected metallic wires. One set of wires is oriented along the direction defined by $\hat{\boldsymbol{u}}_1$, whereas the complementary set is oriented along $\hat{\boldsymbol{u}}_2$. The distance between perpendicular adjacent planes of wires is $a/2$. The plane of incidence is the xoz plane and the incident wave is TM-z polarized [$\boldsymbol{k}^{inc} = (k_x, 0, k_z^{inc})$, $\boldsymbol{H}^{inc} = H^{inc}\hat{\boldsymbol{u}}_y$].

tive possibilities to achieve negative refraction using, for example, indefinite anisotropic materials [5–11] or photonic crystals [12,13].

Recently, we have suggested a novel route to obtain all-angle broadband negative refraction based on materials with spatial dispersion. In Ref. [14], following some earlier studies [15,16], it was shown that due to the strongly nonlocal electromagnetic response of a crossed wire mesh (double wire medium), it is possible to bend the impinging light rays in an unusual manner and obtain broadband negative refraction. Specifically, the emergence of negative refraction in the crossed wire mesh can be intuitively understood by noting that each array of parallel wires provides a different channel of propagation for the incoming wave, and that the dominant channel of propagation is such that the angle of refraction of the energy flow is negative. This novel approach to negative refraction is quite different from negative refraction by double-negative media, photonic crystals, or even indefinite anisotropic materials.

In this work we further study the phenomenon of negative refraction in a crossed wire mesh, and investigate the possibility of taking advantage of this effect to obtain partial focusing with a flat lens.

The paper is organized as follows. In Section 2, the geometry of the metamaterial and the corresponding homogenization model are described. In Section 3, we provide the guidelines for the design of a planar crossed wires lens. Next, in Section 4 we numerically study the imaging of a magnetic line source by the proposed lens. Finally, in Section 5 the conclusion is drawn.

In this work the fields are assumed monochromatic with time dependence $e^{j\omega t}$.

2. Homogenization model

The metamaterial considered here consists of a crossed wire mesh of nonconnected metallic wires with radius r_w and arranged in a square lattice with lattice constant a. The two arrays of parallel wires are orthogonal to each other and are placed at a distance of $a/2$ from each other. The orientation of the two wire arrays is determined by the perpendicular unit vectors $\hat{\boldsymbol{u}}_1 = (1, 0, 1)/\sqrt{2}$ and $\hat{\boldsymbol{u}}_2 = (1, 0, -1)/\sqrt{2}$ (Fig. 1). The wires are embedded in a dielectric with relative permittivity ε_h and thickness L.

As explained in Refs. [15–18] and described in our previous work [14], in the long wavelength regime the "double wire medium" can be analyzed using homogenization techniques, and is characterized by the following dielectric function

$$\bar{\bar{\varepsilon}}_{eff} = \varepsilon_h \left(\hat{\boldsymbol{u}}_y\hat{\boldsymbol{u}}_y + \varepsilon_{11}\hat{\boldsymbol{u}}_1\hat{\boldsymbol{u}}_1 + \varepsilon_{22}\hat{\boldsymbol{u}}_2\hat{\boldsymbol{u}}_2\right). \tag{1}$$

The permittivity components ε_{11} and ε_{22} are given by

$$\varepsilon_{ii}(\omega, k_i) = 1 - \frac{\beta_p^2}{\varepsilon_h(\omega/c)^2 - k_i^2}, \quad i = 1, 2 \tag{2}$$

where c is the speed of light in vacuum, $\boldsymbol{k} = (k_x, k_y, k_z)$ is the wave vector, $k_i = \boldsymbol{k}.\hat{\boldsymbol{u}}_i$, and $\beta_p = [2\pi/(\ln(a/2\pi r_w) + 0.5275)]^{1/2}/a$ is the plasma wavenumber.

Before considering the more complicated problem of radiation of a source above the metamaterial lens, let us concentrate first on the analysis of a simple plane wave scattering problem such that the incident wave vector is in the xoz plane ($k_y = 0$) and the incoming magnetic field is polarized along the y direction, as illustrated in Fig. 1. It was shown in Ref. [14] that the dispersion characteristic of the plane wave modes supported by the structured material for this specific polarization is equivalent to a polynomial equation of third degree in the variable k_z^2. Thus, the homogenization model predicts that the crossed wire mesh supports three independent plane wave modes with the magnetic field along the y direction, an effect which is only possible because of the

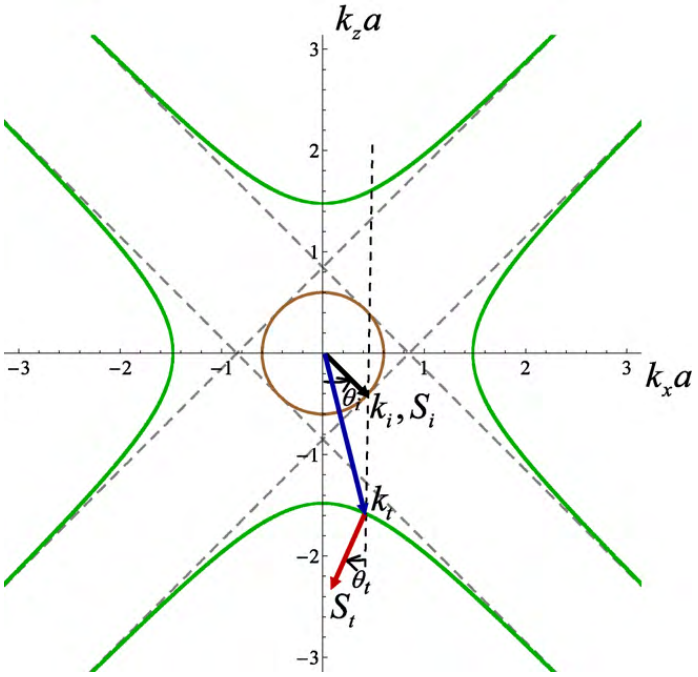

Fig. 2. Isofrequency contour of the fundamental plane wave mode supported by the crossed wire mesh (Fig. 1) for the normalized frequency $\omega a/c = 0.6$, $\varepsilon_h = 1$ and $r_w = 0.05a$ (green lines), as well as the isofrequency contour in the air region (brown circle). The gray dashed lines represent the asymptotes of the two hyperbolas. The transmitted wave vector k_t (blue arrow) is determined by the conservation of the tangential component of the wave vector k_x at the interface, whereas the Poynting vector S_t (red arrow) is normal to the isofrequency curves and is oriented towards increasing frequencies. (For interpretation of the references to color in this figure legend, the reader is referred to the web version of the article.)

strongly nonlocal response of the metamaterial, since for conventional local materials each fixed polarization is associated with a single plane wave.

Here, we write the magnetic field in the three regions of space as follows (the x dependence and the time variation $e^{j\omega t}$ of the fields are suppressed),

$$\begin{aligned} H_y^{(1)} &= H_y^{inc}(e^{\gamma_0 z} + Re^{-\gamma_0 z}), \quad z > 0 \\ H_y^{(2)} &= A_1^+ e^{-jk_z^{(1)} z} + A_1^- e^{+jk_z^{(1)} z} + A_2^+ e^{-jk_z^{(2)} z} + A_2^- e^{+jk_z^{(2)} z} + A_3^+ e^{-jk_z^{(3)} z} + A_3^- e^{+jk_z^{(3)} z}, \quad -L < z < 0 \\ H_y^{(3)} &= H_y^{\mathrm{inc}} T e^{\gamma_0 (z+L)}, \quad z < -L \end{aligned} \tag{3}$$

In the above, H_y^{inc} is the incident field, $\gamma_0 = \sqrt{k_x^2 - \omega^2 \varepsilon_0 \mu_0}$ is the free space propagation constant, $k_x = \omega\sqrt{\varepsilon_0 \mu_0}\sin\theta_i$, being θ_i the angle of incidence, and R and T are the reflection and transmission coefficients, respectively. The propagation constants $k_z^{(1,2,3)}$ [calculated by solving Eq. (5) of Ref. [14] with respect to k_z] and the amplitudes $A_{1,2,3}^{\pm}$ are associated with the electromagnetic modes excited inside the metamaterial slab. For each plane wave with magnetic field of the form $\boldsymbol{H} = H_0 e^{-j\boldsymbol{k}.\boldsymbol{r}}\hat{\boldsymbol{u}}_y$, the corresponding electric field is given by

$$\boldsymbol{E} = \frac{H_0}{\omega\varepsilon_0\varepsilon_h}\left(\frac{-k_2}{\varepsilon_{11}}\hat{\boldsymbol{u}}_1 + \frac{k_1}{\varepsilon_{22}}\hat{\boldsymbol{u}}_2\right) e^{-j\boldsymbol{k}.\boldsymbol{r}}. \tag{4}$$

In order to calculate the reflection and transmission coefficients, it is necessary to impose the following boundary conditions:

$$E_x \text{ and } H_y \text{ are continuous at } z = -L \text{ and } z = 0, \tag{5a}$$

$$\boldsymbol{J}_{d,\mathrm{av}}.\hat{\boldsymbol{u}}_1 = 0, \quad \boldsymbol{J}_{d,\mathrm{av}}.\hat{\boldsymbol{u}}_2 = 0 \text{ at } z = -L^+ \text{ and } z = 0^- \tag{5b}$$

The first set of boundary conditions corresponds to the classical boundary conditions which impose that the tangential electric and magnetic fields are continuous at the interfaces. The second set corresponds to the so-called additional boundary conditions (ABCs) introduced in Refs. [19,20], and guarantee that the electric current that flows along each individual metallic wire vanishes at both interfaces [for the definition of the averaged current $\mathbf{J}_{d,\mathrm{av}}$ in Eq. (5b) the reader is referred to Ref. [20]]. These additional boundary conditions are necessary to

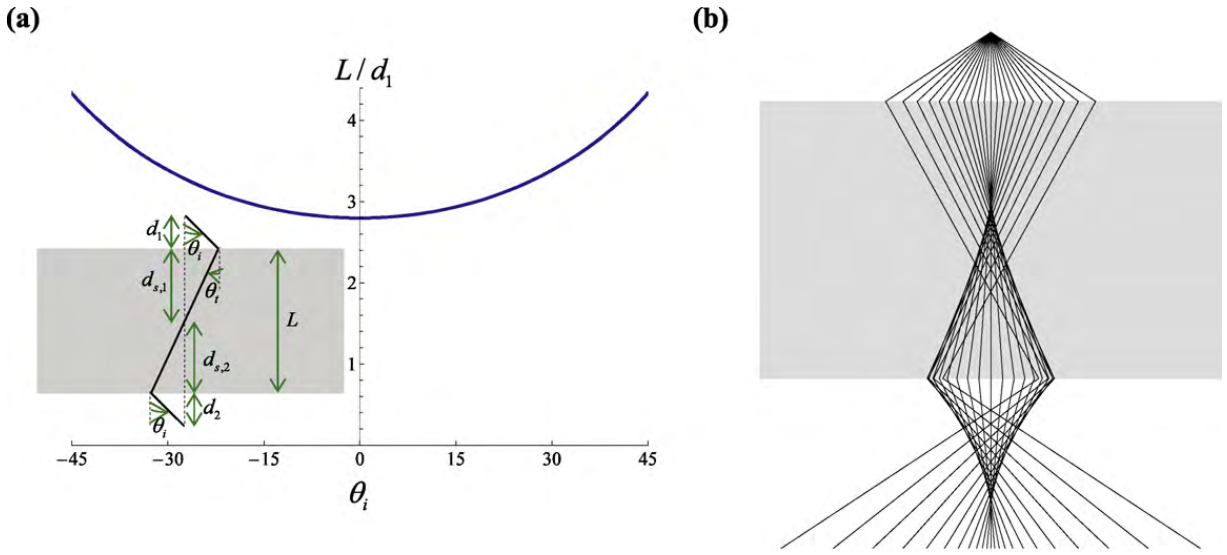

Fig. 3. (a) Normalized thickness of the metamaterial slab as a function of the angle of incidence calculated in order that $d_1 = d_2$. The frequency of operation is $\omega a/c = 0.6$, the radius of the wires is $r_w = 0.05a$, and the permittivity of the host is $\varepsilon_h = 1$. The inset represents the geometry of the problem. (b) Ray-tracing diagram showing that the structured material refocuses the rays coming from a line source both inside and outside the slab. The rays represent the direction of the Poynting vector (energy flow). The source is placed at distance $d_1 = 0.25\,L$ from the front interface and the thickness of the slab is $L = 20a$.

remove the degrees of freedom characteristic of spatially dispersive materials, which are manifested through the existence of "additional waves". In this manner, the scattering problem is reduced to an 8×8 linear system, which can be easily numerically solved (see Ref. [20] for further details).

3. Guidelines for the design of the flat lens

As described in our previous work [14] (see also [15,16,20]), the key ingredient for the emergence of negative refraction is the fact that the crossed wire mesh supports, for propagation in the (xoz) plane (Fig. 1) and long wavelengths, an electromagnetic mode with hyperbolic shaped isofrequency contours (Fig. 2). Hence, as illustrated in Fig. 2, this electromagnetic mode undergoes negative refraction at the interfaces with air. One can easily see that the Poynting vector (energy flow) is always negatively refracted for any incident wave vector (or angle of incidence) since it must be normal to the isofrequency contours. On the other hand, the transmitted wave vector is positively refracted, making an acute angle with the Poynting vector as in indefinite media.

Despite some similarities between these isofrequency contours and those of indefinite materials, there is an evident and significant difference between them. As already explained in Ref. [14], the isofrequency contours of a conventional indefinite anisotropic material consist of a single hyperbola and hence only yield negative refraction when the interface is normal to the principal axis along which the permittivity is negative. On the other hand, the isofrequency contour of the considered spatially dispersive material consists of two hyperbolas with asymptotes running along the directions $\hat{\boldsymbol{u}}_1$ and $\hat{\boldsymbol{u}}_2$ (see Fig. 2), and consequently enables negative refraction if the interface is normal either to the x or to the z direction. Moreover, as mentioned in Section 1, the mechanism that yields negative refraction in the crossed wire mesh is based on the existence of two "propagation channels" (each associated with a different set of parallel wires), and thus is fundamentally different from the mechanism exploited in indefinite materials. Here, we will focus our attention in the study of wave propagation when the interface is normal to the z direction.

In order to study the possibility of partial focusing, we suppose that a line source is placed at a distance d_1 from the front interface of the metamaterial slab (inset of Fig. 3a), and we investigate what is the required thickness L for the slab in order that the radiation of the source is refocused to a point located at a distance $d_1 = d_2$ from the back interface. In general, this thickness depends on the angle of incidence θ_i.

From the inset of Fig. 3a and using simple geometrical arguments, it is straightforward obtain the following equations:

$$d_1\,|\tan\theta_i| = d_{s,1}\,|\tan\theta_t| \tag{6a}$$

$$d_2\,|\tan\theta_i| = (L - d_{s,1})\,|\tan\theta_t| \tag{6b}$$

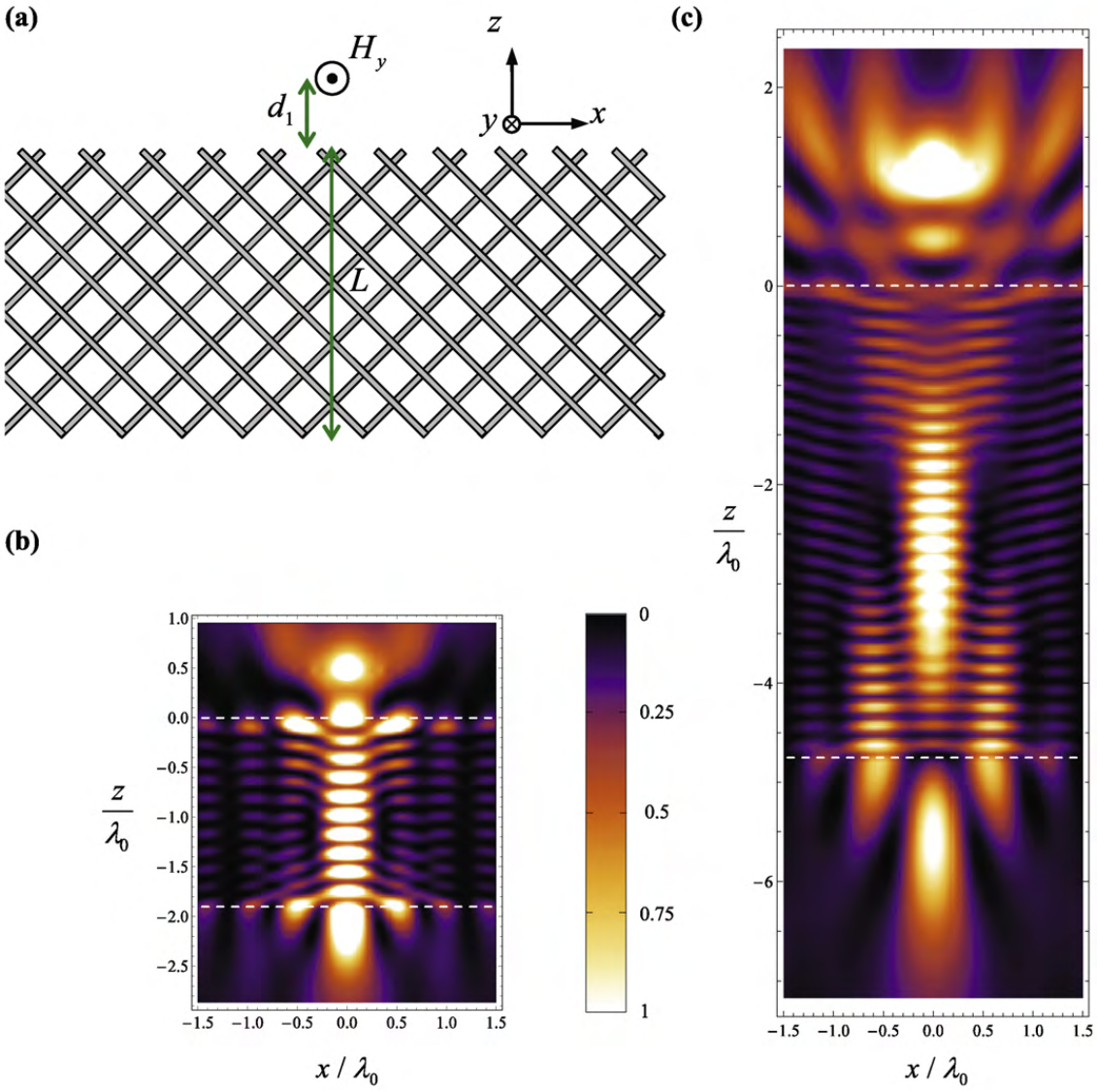

Fig. 4. (a): Geometry of the problem: a magnetic line source is placed at a distance d_1 above the crossed wires lens. (b) and (c): Squared (normalized) amplitude of the magnetic field $|\mathbf{H}|^2$. The frequency of operation is $\omega a/c = 0.6$, the radius of the wires is $r_w = 0.05a$, the permittivity of the host is $\varepsilon_h = 1$, and the source is located at a distance $d_1 = 0.25\,L$ from the front interface of the slab. The white dashed lines represent the interfaces of the slab. (b) $L = 20a$; (c) $L = 50a$.

The angle θ_t represents the angle of refraction of the energy flow (determined by Poynting vector of the transmitted wave) and is calculated using the relation $v_g = \nabla_k \omega(\boldsymbol{k})$. Then, substituting Eq. (6a) in Eq. (6b) and considering that $d_1 = d_2$ we easily obtain the following formula for the normalized thickness of the slab L

$$\frac{L}{d_1} = 2\left|\frac{\tan\theta_i}{\tan\theta_t}\right| \tag{7}$$

In Fig. 3a we depict the required normalized thickness for the slab as function of the angle of incidence, calculated using Eq. (7).

As seen the required thickness for the slab is not constant and depends on the angle of incidence. This was expected, since as demonstrated in Ref. [14], the angle of transmission θ_t is a nonlinear function of θ_i. Hence, unlike what happens in Pendry's lens where $\theta_t = \theta_i$ and consequently the thickness $L = 2d_1$ provides perfect focusing, this structured slab does not possess pairs of pure aplanatic points [21]. Nevertheless, despite this non-ideal characteristic, the proposed lens may enable a partial focusing of the radiation somehow similar to what is achieved using a flat slab of indefinite anisotropic material [6,10]. Clearly, from Fig. 3a, the thickness of the slab should be chosen so that $L > 2.8d_1$ to ensure that $d_1 \approx d_2$. To illustrate the possibilities, we depict in Fig. 3b the ray-tracing diagram showing the path of the rays inside and outside the slab for $d_1 = 0.25L$. It is seen that the rays coming from the line source (located above the slab) are partially refocused inside the slab, and also

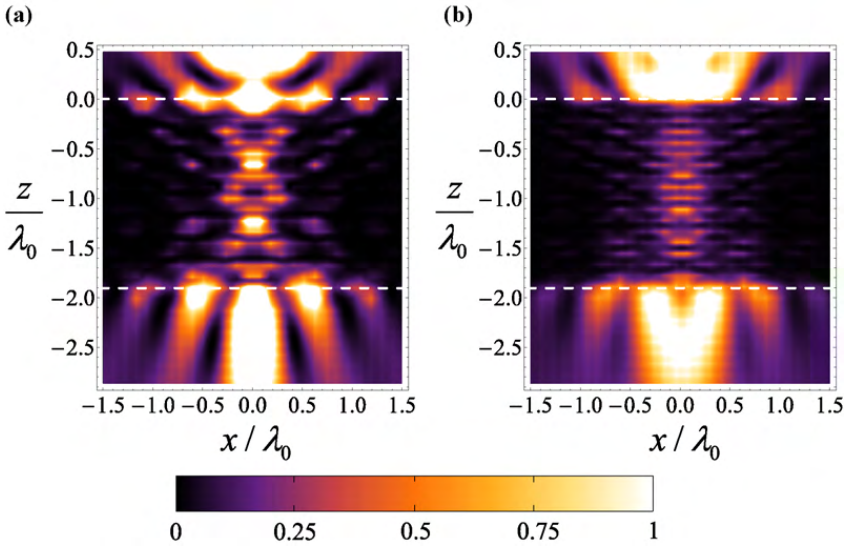

Fig. 5. Normalized $|\mathbf{H}|^2$ (a) and $|\mathbf{E}|^2$ (b) for an array of crossed wires with thickness $L = 20a$, radius of the wires $r_w = 0.05a$, and permittivity of the host $\varepsilon_h = 1$. The magnetic line source is placed at distance $d_1 = 0.25\,L$ from the front interface of the slab. The frequency of operation is $\omega a/c = 0.6$.

after crossing the metamaterial lens at a partial focus located at a distance $d_1 \approx d_2$. Other numerical tests that we have done suggest that $d_1 = 0.25\,L$ is a good compromise solution, which despite the non-ideality of the lens yields a well-defined focus at the image plane.

4. Imaging a line source

In order to verify the results discussed in the previous section and characterize the effects of diffraction, here we consider the scenario where a magnetic line source (infinitely extended along y direction) is placed at a distance d_1 above the crossed wires slab (Fig. 4a). The magnetic field radiated by the line source is of the form $H_y = A(1/4j)H_0^{(2)}(\omega/c \cdot \rho)$, where A is some constant that depends on the line current, ρ is the radial distance to the source, and $H_0^{(2)} = J_0 - jY_0$ is the Hankel function of second kind and order zero. Assuming that the metamaterial slab is unbounded along the directions x and y, it is straightforward to show that the magnetic field in the three regions of space can be written in terms of the Sommerfeld-type integrals:

$$
\begin{aligned}
H_y^{(1)}(x,z) &= \frac{A}{\pi}\int_0^\infty \frac{1}{2\gamma_0}\left(e^{-\gamma_0|z-d_1|} + R(\omega,k_x)e^{-\gamma_0(z+d_1)}\right)\cos(k_x x)dk_x, \quad z>0\\
H_y^{(2)}(x,z) &= \frac{A}{\pi}\int_0^\infty \frac{1}{2\gamma_0}H_y^{(2)}(k_x,z)e^{-\gamma_0 d_1}\cos(k_x x)dk_x, \quad -L<z<0\\
H_y^{(3)}(x,z) &= \frac{A}{\pi}\int_0^\infty \frac{1}{2\gamma_0}T(\omega,k_x)e^{\gamma_0(z+L-d_1)}\cos(k_x x)dk_x, \quad z<-L
\end{aligned}
\tag{8}
$$

where $H_y^{(2)}(k_x,z)$ is the magnetic field inside the slab ($-L<z<0$) defined in Eq. (3), and $R(\omega,k_x)$ and $T(\omega,k_x)$ are the reflection and transmission coefficients obtained by solving the plane wave scattering problem. Using the above formulas we have calculated the magnetic field profile in all regions of space.

In Fig. 4b and c the density plots of $|\mathbf{H}|^2$ are depicted in the xoz plane for the configuration illustrated in Fig. 4a with $d_1 = 0.25\,L$. In both figures it is clearly seen an intense partial focus of the magnetic field inside the crossed wires lens, and also behind the lens. Hence, these results confirm the findings of Section 3, and prove that a flat slab of nonconnected crossed wires can indeed redirect the electromagnetic radiation of a p-polarized line source (such that the electric field is in the plane of the wires) to a narrow spot at the focal plane.

It is seen in Fig. 4b that for a slab with thickness $L = 20a$ the focal point behind the lens spreads somehow along the z direction, and partially overlaps the back interface of the slab. In order to achieve a focal point clearly detached from the interface, we can use a slab with larger thickness L, as shown in Fig. 4c, for a lens with $L = 50a$. This can be understood by noting that for a fixed frequency of operation, the characteristic dimension of the system as compared to the wavelength increases with L, and thus the laws of geometrical optics and the ray-tracing analysis become more accurate (or in other words, the effects of wave diffraction are miti-

gated). Furthermore, it is noticeable in Fig. 4c that the focal region is somehow elongated, consistent with the ray-tracing analysis of Fig. 3b, as a consequence of the fact that the angle of refraction θ_t inside the lens is angle-dependent, as already discussed in Section 3.

In the region above the slab of crossed wires (where the source is located) some effects of reflections can be detected. Indeed, there is some mismatch between the impedances of the structured material and free space, because the effective impedance of the metamaterial is relatively low [14].

The half-power beamwidth measured at the focal plane for the example reported in Fig. 4c is $0.4\lambda_0$, similar to the conventional diffraction limit value ($\lambda_0/2$).

The results described above were obtained using the analytical model (Eq. (8)), and assume that the metamaterial slab is infinitely extended along the x and y directions. In order to confirm these homogenization results and also the ray-tracing diagram (Fig. 3b), we used a homemade Method of Moments (MoM) code to numerically simulate the focusing properties of a finite width metamaterial slab illuminated by a magnetic line source. The MoM code takes into account all the fine details of the microstructure of the artificial material. In the MoM simulation the structured material slab is periodic along the y direction, and finite along the x direction with width W. It is assumed that each plane of wires (parallel to xoz plane) is formed by 100 wires, so that the width of the slab is approximately $W = 100a\sqrt{2}$.

The spatial maps of the normalized squared amplitude of the magnetic and electric fields calculated with the MoM are shown in Fig. 5. An intense partial focus of the magnetic field (Fig. 5a) on the far side of the slab relative to the line source is clearly seen, confirming the homogenization results and further demonstrating that this structure works, indeed, as a planar focusing device. Contrary to what happens with the intensity of the magnetic field, the intensity of the electric field (Fig. 5b) inside the metamaterial slab is significantly weaker than in the free space regions [14]. Indeed, as mentioned before, the crossed wire mesh is a low impedance material. Due to this property, which implies some impedance mismatch with free space, some reflections can be detected in the region above the first interface, consistent with the results of the analytical model.

5. Conclusion

In conclusion, we have demonstrated that a spatially dispersive material formed by nonconnected crossed metallic wires may be used as a planar lens that focuses electromagnetic radiation in a narrow spot both behind the lens and inside the lens. The spot size width at the focal plane is near $\lambda_0/2$ (diffraction limit), similar to the resolution obtained with a planar lens formed by an anisotropic indefinite material. Despite some similarities of the reported focusing effect and the results achievable using an indefinite anisotropic material, its physical origin is completely distinct. In the crossed wire mesh the hyperbolic isofrequency contours are rooted on the existence of two "propagation channels", each associated with a different array of wires, whereas in indefinite media it is related to the sign of the principal elements of the permittivity and permeability tensors.

Acknowledgments

This work was funded by Fundação para Ciência e a Tecnologia under project PTDC/EEA-TEL/100245/2008. T.M. acknowledges financial support by Fundação para a Ciência e a Tecnologia under the fellowship SFRH/BD/37876/2007.

References

[1] V.G. Veselago, Sov. Phys. Usp. 10 (1968) 509.
[2] J.B. Pendry, Phys. Rev. Lett. 85 (2000) 3966.
[3] R.A. Shelby, D.R. Smith, S. Schultz, Science 292 (2001) 77.
[4] J. Valentine, S. Zhang, T. Zentgraf, E. Ulin-Avila, D.A. Genov, G. Bartal, X. Zhang, Nature (London) 455 (2008) 376.
[5] D.R. Smith, D. Schurig, Phys. Rev. Lett. 90 (2003) 077405.
[6] D.R. Smith, D. Schurig, J.J. Mock, P. Kolinko, P. Rye, Appl. Phys. Lett. 84 (2004) 2244.
[7] X. Fan, G.P. Wang, J.C.W. Lee, C.T. Chan, Phys. Rev. Lett. 97 (2006) 073901.
[8] A.J. Hoffman, L. Alekseyev, S.S. Howard, K.J. Franz, D. Wasserman, V.A. Podolskiy, E.E. Narimanov, D.L. Sivco, G. Gmachl, Nature Mater. 6 (2007) 946.
[9] J. Yao, Z. Liu, Y. Liu, Y. Wang, C. Sun, G. Bartal, A.M. Stacy, X. Zhang, Science 321 (2008) 930.
[10] Y. Liu, G. Bartal, X. Zhang, Opt. Exp. 16 (2008) 15439.
[11] A. Fang, T. Koschny, C.M. Soukoulis, Phys. Rev. B 79 (2009) 245127.
[12] M. Notomi, Phys. Rev. B 62 (2000) 10696.
[13] E. Cubukcu, K. Aydin, E. Ozbay, S. Foteinopoulou, C.M. Soukoulis, Nature (London) 423 (2003) 604.
[14] M.G. Silveirinha, Phys. Rev. B 79 (2009) 153109.
[15] M.G. Silveirinha, C.A. Fernandes, IEEE Trans. Microwave Theory Tech. 53 (2005) 1418.
[16] C.R. Simovski, P.A. Belov, Phys. Rev. E 70 (2004) 046616.
[17] I.S. Nefedov, A.J. Viitanen, S.A. Tretyakov, Phys. Rev. B 72 (2005) 245113.
[18] M.G. Silveirinha, C.A. Fernandes, Phys. Rev. B 78 (2008) 033108.
[19] M.G. Silveirinha, C.A. Fernandes, J. Costa, New J. Phys. 10 (2008) 053011.
[20] M.G. Silveirinha, New J. Phys 11 (2009) 113016.
[21] M. Born, E. Wolf, Principles of Optics, 6th ed., Pergamon Press, Oxford, 1993.